

Aging in short-ranged attractive colloids: A numerical study

G. Foffi^{a)} and E. Zaccarelli

Dipartimento di Fisica and INFM Center for Statistical Mechanics and Complexity, Università di Roma "La Sapienza," Piazzale Aldo Moro 2, 00185 Roma, Italy

S. Buldyrev

Center for Polymer Studies and Department of Physics, Boston University, Boston, Massachusetts 02215

F. Sciortino and P. Tartaglia

Dipartimento di Fisica and INFM Center for Statistical Mechanics and Complexity, Università di Roma "La Sapienza," Piazzale Aldo Moro 2, 00185 Roma, Italy

(Received 1 December 2003; accepted 12 February 2004)

We study the aging dynamics in a model for dense simple liquids, in which particles interact through a hard-core repulsion complemented by a short-ranged attractive potential, of the kind found in colloidal suspensions. In this system, at large packing fractions, kinetically arrested disordered states can be created both on cooling (attractive glass) and on heating (repulsive glass). The possibility of having two distinct glasses, at the same packing fraction, with two different dynamics offers the unique possibility of comparing—within the same model—the differences in aging dynamics. We find that, while the aging dynamics of the repulsive glass is similar to the one observed in atomic and molecular systems, the aging dynamics of the attractive glass shows novel unexpected features.

© 2004 American Institute of Physics. [DOI: 10.1063/1.1695326]

I. INTRODUCTION

In the last years, the physics of systems characterized by short-ranged attractive interparticle interactions—short in comparison to the particle size—has been the focus of several investigations. A good example of this type of systems are colloidal solutions, since the intensity and the range of the potential can be finely controlled by changing the solvent properties or the chemistry of the dispersed particles. The short range of the attractive interaction produces thermodynamic features which are not observed in atomic or molecular system (where the interaction range is always long ranged).^{1–4} Recently, theoretical, numerical and experimental studies have focused on the dynamical properties of these systems. One of the most astonishing discovery is that, at high density, the metastable liquid is characterized by a non-monotonic temperature dependence of the characteristic structural times: The dynamics slows down not only upon cooling (as commonly observed in molecular systems), but also upon heating. The slowing down upon heating can be so intense that a novel mechanism of arrest takes place high T .⁵ In the high density part of the phase diagram, for sufficiently short-ranged potentials, a re-entrant liquid–glass line is observed and a liquid phase emerges between two glasses. In other words, moving along a constant density path, it is possible to pass from a glass phase to a liquid phase and then again in a new glass phase just by progressively lowering the temperature. The two glasses are named “attractive glass” and “repulsive glass” due to the different mechanisms, respectively, attraction and excluded volume, which control the dynamical slowing down.⁶ In the re-entrant liquid region, between the attractive and repulsive glasses, dynamics is

very unusual. Correlation functions show a subtle logarithmic decay, while the particle mean-squared displacement follows a power-law in time.

The complex dynamics in short-ranged attractive systems has been interpreted within mode coupling theory (MCT).⁷ Theoretical predictions do not depend on the detailed shape of the attractive potential and have been confirmed for many different modelization of the attractive tail.^{8–12} A set of simulations^{13–16} and experiments^{17–22} have confirmed the existence of such complex dynamics.

In numerical work based on the square well system (SWS), one of the simplest models studied, it has been shown that a diffusivity maximum in temperature appears when the width of the square well is short enough compared to the hard-core diameter.¹⁵ The calculation of the iso-diffusivity lines in equilibrium¹⁴ confirms the reentrant behavior and the novel dynamics which take place in the reentrant region. Along an iso-diffusivity path, the decay of the density–density correlation functions, which at high temperature can be well described by a stretched exponential, becomes more and more uncommon upon cooling, showing at low T signs of logarithmic decay.^{13,15,23}

Previous numerical work has focused on equilibrium properties and on the dynamics near the predicted glass–glass transition.^{13–15,24} Here we report a study of the non-equilibrium dynamics. Starting from an equilibrium state in the re-entrant fluid region, the system is quenched both at low and high temperature. We are then able to explore—within the same model—the aging dynamics for the attractive and repulsive glass, to find out if the differences which characterize the dynamics in the glassy state show up also in the out-of-equilibrium evolution. We discover that, while the aging dynamics of the repulsive glass is similar to the one

^{a)}Electronic mail: giuseppe.foffi@phys.uniroma1.it

observed in atomic and molecular liquids,^{25,26} the aging dynamics of the attractive glass shows novel unexpected features. We also report comparison with a recent experimental study of aging in short-ranged colloidal systems.²⁷

II. SIMULATION DETAILS

We investigate a system that has been extensively studied earlier in the equilibrium regime, a binary square well mixture.¹⁵ The binary system is a 50%–50% mixture of $N = 700$ particles. The two species (labeled A and B) are characterized by a diameter ratio $\delta = \sigma_A/\sigma_B = 1.2$. Masses are chosen to be equal and unitary. The attraction is modeled by a square well interaction defined according to

$$V_{ij}(r) = \begin{cases} \infty & r_{ij} < \sigma_{ij} \\ -u_0 & \sigma_{ij} < r_{ij} < \sigma_{ij} + \Delta_{ij} \\ 0 & r_{ij} > \sigma_{ij} + \Delta_{ij}, \end{cases} \quad (1)$$

where $\sigma_{ij} = (\sigma_i + \sigma_j)/2$, $i, j = A, B$ and Δ_{ij} has been chosen in such a way that $\epsilon_{ij} = \Delta_{ij}/(d_{ij} + \Delta_{ij}) = 0.03$. We choose $k_B = 1$ and the depth of the potential $u_0 = 1$. Hence $T = 1$ corresponds to a thermal energy equal to the attractive well depth. The diameter of the small specie is chosen as unity of length, i.e., $\sigma_B = 1$. Density is parametrized in terms of packing fraction $\phi = (\rho_A d_A^3 + \rho_B d_B^3) \cdot \pi/6$, where $\rho_i = N_i/L^3$, L being the box size and N_i the number of particles for each species. Time is measured in units of $\sigma_B \cdot (m/u_0)^{1/2}$. The unit has been chosen consistently with Ref. 15, where the same system has been studied in equilibrium. A standard MD algorithm has been implemented for particles interacting with SWS potentials.²⁸ Between collisions, particles move along straight lines with constant velocities. When the distance between the particles becomes equal to the distance where $V(r)$ has a discontinuity, the velocities of the interacting particles instantaneously change. The algorithm calculates the shortest collision time in the system and propagate the trajectory from one collision to the next one. Calculations of the next collision time are optimized by dividing the system in small subsystems, so that collision times are computed only between particles in the neighboring subsystems.

With the present choice of parameters, the formation of crystallites during the simulation run is not observed. As compared to the monodisperse case, the slight asymmetry in the diameters allows us to follow the development of the slow dynamics over several orders of magnitude.¹⁴ We choose to work at the packing fraction $\phi = 0.608$, being this density in the middle of the re-entrant region of the phase diagram, as shown in previous calculations.¹⁵ At this density we prepared 60 independent configurations, equilibrated at the initial temperature $T_i = 0.6$. Subsequently we quenched these independent configurations to the desired final temperatures, and then we followed the evolution in time at constant temperature. The characteristic time of the thermostat as been chosen to be much smaller than the structural relaxation time and such that the system may equilibrate within one time unit. Each of the 60 independent configurations has been quenched to $T_f = 1.2$, i.e., in the repulsive glass, and to $T_f = 0.3$, i.e., in the attractive glass and run up to $t_f = 2 \times 10^5$. The numerical protocol is illustrated in Fig. 1. Iso-

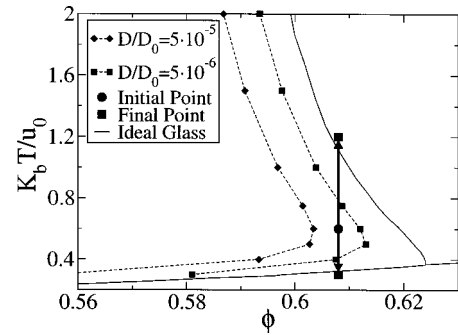


FIG. 1. Square well iso-diffusivity curves (i.e., the locus of points in the ϕ, T plane where the normalized diffusion coefficient is constant) for three different values of D/D_0 ($D_0 = \sigma_b \sqrt{T}/m$ data from Ref. 39). The extrapolated ideal glass line is also reported (data from Ref. 23). Equilibrium starting configurations at $\phi = 0.608$ and $T_i = 0.6$ (filled circle) are instantaneously quenched at $t = 0$ to $T_f = 0.3$ and $T_f = 1.2$ (plus).

diffusivity curves from Ref. 15 and the extrapolated ideal glass line from Ref. 23 are plotted together with the quench path selected in this work. Since the system, after the quench, is out of equilibrium, all averages—represented in the text by the symbol $\langle \cdot \rangle$ —have been performed over the ensemble of the 60 initial independent configurations.

III. RESULTS AND DISCUSSION

Numerical investigations of aging in glassy materials are usually accomplished by rapidly quenching the system from an equilibrium state to a new state, where the characteristic time scale of the structural relaxation is much longer than the observation time. When the time scale of the final state exceeds the characteristic time of the simulation, equilibrium cannot be reached within the simulation time. Out of equilibrium time translation invariance does not hold and the state of the system does not only depend from the external parameters, but also from the time elapsed from the quench, the so-called waiting time t_w . Indeed in the aging regime other notable effects emerge, i.e., violation of the fluctuation dissipation theorem^{29–33} and strong dependence on the story of the system.²⁵ Thus, in out-of-equilibrium conditions correlation functions will depend both on the time of observation t and on the waiting time t_w , i.e., $C_A(t_w, t) = \langle A^*(t_w) A(t_w + t) \rangle$. Similarly, the one time properties (e.g., the static structure factor or the energy), will depend on the waiting time t_w .

The first quantity that we investigate is the average potential energy of the system U . At $t_w = 0^+$, i.e., instantaneously after the quenches to, respectively, $T_f = 1.2$ and $T_f = 0.3$, the two systems possess the same potential energy. Then, with t_w , they start evolving toward different energy values. The situation is represented in Fig. 2. While the system quenched to $T_f = 1.2$, i.e., in the repulsive regime, shows an increase in the potential energy (i.e., a progressive breaking of the interparticle bonding), the one quenched to $T_f = 0.3$ shows the opposite behavior. In both cases, the time dependence of the potential energy shows a fast short-time ($t_w < 1$) evolution (which reflects the equilibration of the fast degrees of freedom) followed by a much slower evolution, proper of the aging dynamics. The aging dynamics has de-

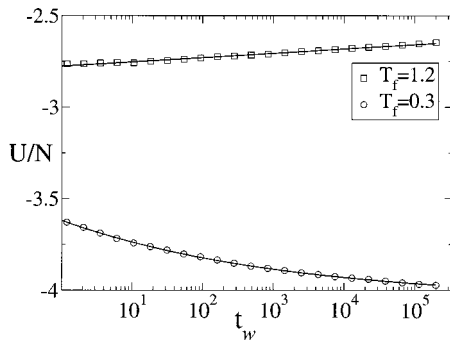


FIG. 2. Average potential energy U after the quench as function of the time t_w elapsed from the quench. The symbols are the simulation data and the continuous line are the fits. Data for $t_w < 1$ are not shown since the kinetic energy has not yet equilibrated to the final value. For $T_f = 1.2$ the fit is $U/N = -2.77 + 0.01 \ln(t_w)$ while for $T_f = 0.3$ we obtain $U/N = -4.05 + 0.43 t_w^{-0.14}$

tectable different trends at high and low temperatures. While at high temperatures a clear $\log(t_w)$ dependence of U is observed, at low T the time dependence in log scale is not linear and can be well fitted by $U - U_{\text{eq}} \sim t_w^{-a}$, with $a \approx 0.14$. A similar form was successfully adopted by Parisi for a binary system of soft spheres in the aging regime.³⁰ The time evolution of the aging structure can be followed by numerical calculation of the partial static structure factors, $S_{\alpha\beta}(q, t_w)$ defined as

$$S_{\alpha\beta}(q, t_w) = (\varrho_{\alpha}^*(\mathbf{q}, t_w) \varrho_{\beta}(\mathbf{q}, t_w) / \sqrt{n_{\alpha} n_{\beta}}), \quad (2)$$

where the partial density variables are defined as $\varrho_{\alpha}(\mathbf{q}) = \sum_k \exp[i\mathbf{q} \cdot \mathbf{r}(t)_k^{(\alpha)}] / \sqrt{N}$, and $n_i = N_i / N$ are the partial concentrations. In equilibrium, time translation invariance implies $S_{\alpha\beta}(q, t) = S_{\alpha\beta}(q, 0)$, i.e., the static structure factor is a time independent function.

The inset of Fig. 3 shows $S_{AA}(q, t_w)$ for the quench to $T_f = 1.2$, for waiting times spanning four decades. Similarly to binary Lennard-Jones systems,²⁵ the variation of the static structure factor is particularly small, for all α, β components. With increasing t_w a very weak increase at all peaks of the structure factors is observed. This is shown in the main figure. Similarly for the $T_f = 0.3$ case, the $S_{\alpha\beta}(q, t_w)$ changes are very small, as shown in Fig. 4. Interestingly enough, for

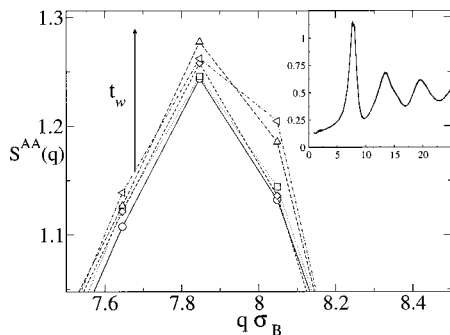


FIG. 3. First peak of the static structure factor at different waiting time t_w , 10^1 (circles), 10^2 (squares), 10^3 (diamonds), 10^4 (triangles up), and 10^5 (triangles left). The quench is at $T_f = 1.2$. For long t_w there is slow growth of the peaks of the structure factors. In the inset structure factors for the same t_w are displayed.

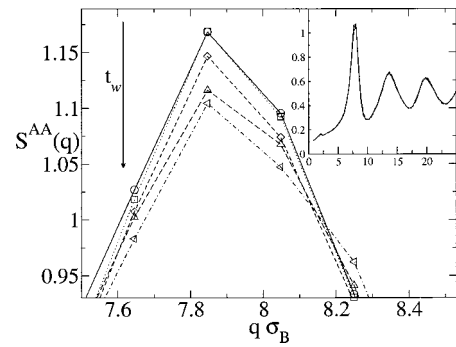


FIG. 4. Same as Fig. 3 for $T_f = 0.3$.

the first peak (and only there) the trend is reverted with respect to the previous case, i.e., the intensity of $S_{AA}(q, t_w)$ around the peak decreases on aging. This observation agrees with equilibrium studies. Indeed, for the square well system, an increase in temperature produces an increase in the first peak toward the hard-sphere limit whereas lowering the temperature only promotes the structure factor oscillations at large wave vector.³⁴ It is perhaps interesting to recall that within MCT, the increase of $S_{\alpha\beta}$ at the first peak is responsible for the formation of the repulsive glass, whereas the long lasting oscillations in the structure factor generates the kinetic arrest in the attractive glass.¹⁰

Next we study the intermediate scattering function, i.e., dynamic density–density correlators. For a binary mixture this quantity is defined by

$$\phi_{\alpha\beta}(q, t, t') = \langle \varrho_{\alpha}(\mathbf{q}, t) \varrho_{\beta}(\mathbf{q}, t') \rangle / S_{\alpha\beta}(q, t'), \quad (3)$$

where the density variables $\varrho_{\alpha}(\mathbf{q}, t)$ have been defined before. In equilibrium $\phi_{\alpha\beta}(q, t, t')$ will depend only on the difference $t - t'$. When the system ages the density–density correlators is a function of t_w and t . In this paper, we show $\phi_{\alpha\beta}(q, t, t')$ as a function of t_w and the time difference $(t - t_w)$, i.e., $\phi_{\alpha\beta}(q, t_w, t - t_w)$. The density correlation is normalized by $S_{\alpha\beta}(q, t_w)$. The upper panel of Fig. 5 shows the t_w dependence of $\phi_{AA}(q, t_w, t - t_w)$, with $q\sigma_B = 8.72$, which lies between the first and the second peak in the static structure factor. On increasing t_w , the decay of the correlation functions becomes slower and slower. The time needed to lose memory of the starting configuration grows. This is a typical feature of aging systems and it has been encountered both in experiments²⁷ and simulations.²⁵ The slowing down of the dynamics on increasing t_w resembles the way the structural arrest emerges in supercooled liquids on approaching the glass transition. Indeed, in this case, upon cooling two characteristic time scales emerge, a fast decay around a plateau value and a slow decay to zero. The time duration of the plateau becomes longer, the closer the system is to the glass transition. On the other hand, in the aging regime the control parameter is the waiting time t_w , which plays a role analogous to that played by T in equilibrium, i.e., the longer t_w the longer is the time requested to lose memory. In the same way as temperature measures the distance from the glass transition in equilibrium liquids, t_w measures the progressive thermalization of the structural degrees of freedom.

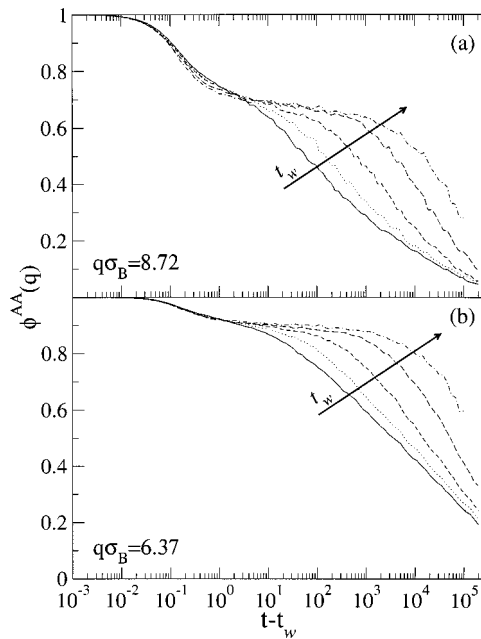


FIG. 5. (a) Density–density correlation function $\phi_{AA}(q, t_w, t-t_w)$ after a quench at $T_f=1.2$ for $q\sigma_B=8.72$. From right to left, longer and longer relaxation time, $t_w=10^1$ (continuous line), 10^2 (dotted line), 10^3 (short-dashed line), 10^4 (long-dashed line), 10^5 (dot-dashed line). (b) Same results but for $q\sigma_B=6.37$.

In summary, with increasing t_w the system develops a clear plateau, whose height is consistent with the value expected for the repulsive glass.

Similar results are shown in the lower panel of Fig. 5 for $q\sigma_B=6.37$, which is close to the maximum of the static structure factor. Two main differences emerge between the correlators at the two wave vectors: (i) The relaxation time is longer for $q\sigma_B=6.37$, (ii) the plateau is higher. Both this issues follow, as expected, the trend of the equilibrium results, where at the maximum of the structure factor a maximum of the relaxation time and of the nonergodicity parameter is encountered.³⁵

The upper panel of Fig. 6 shows the density–density correlation functions for the quench at $T_f=0.3$ for $q\sigma_B=8.72$. Similarly to what we found in the previous case, the time of decay of the correlators grows with the waiting time t_w . However, the shape of the functions is drastically different, confirming that even the aging dynamics reflects the differences noted in the previous equilibrium studies. Two notable differences with the $T_f=1.2$ case are: (i) The strength of the α -relaxation (i.e., the height of the plateau) in aging is much more intense, being now close to one; (ii) the plateau does not significantly stretch in time (as shown in the inset) beyond $t-t_w \approx 1$. Similar trends are found for a q -vector closer to the first peak of the structure factor, as shown in the lower panel of Fig. 6.

A recent study of the glass–glass transition has suggested the possibility that the attractive glass is significantly destabilized by hopping processes,²⁴ which in the present context can be associated with the breaking of the interparticle bonds. The data shown in the inset of Fig. 6 support

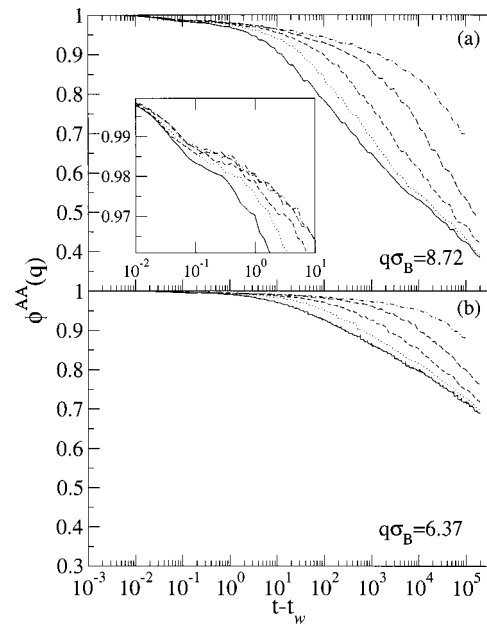


FIG. 6. Same as Fig. 5 but for the quench at $T_f=0.3$. In the inset in (a), an enlargement of the plateau area is shown (see text for details).

such interpretation, since no clear plateau can be observed for $t_w > 1$.

A very interesting feature of the correlation functions in the aging regime is the property of scaling with waiting time. Theoretical studies suggest that correlators at different waiting time can be rescaled by the equation

$$\phi_{\alpha\beta}(q, t_w, t-t_w) = \phi_{\alpha\beta}^{st}(q, t) + \phi_{\alpha\beta} \left(q, \frac{h(t-t_w)}{h(t_w)} \right), \quad (4)$$

where $\phi_{\alpha\beta}^{st}(q, t)$ accounts for the short time.³⁶ The $h(t)=t$ case is the so-called simple aging case. For a binary mixture of Lennard-Jones spheres the system follows (4) with $h(t)=t^\alpha$ and $\alpha \approx 0.88$.²⁵ Similar results have been also found in a numerical study of aging in a soft-spheres binary mixtures.³⁷

We tried to apply this scaling relation to our system. We focus on the low temperature quench, since the high temperature one shows a phenomenology, which is similar to the Lennard-Jones case. In the case of aging of $T_f=0.3$ no clear scaling of the correlation functions can be performed. In Fig. 7(a) we show the crude tentative of data scaling. Correlators have been shifted in time to superimpose the correlators in the region where $0.7 < \phi_q < 0.9$. Figure 7(b) shows the same data, this time shifted to maximize superposition for $0.35 < \phi_q < 0.5$. In Fig. 8 the scaling coefficients t_r used to obtain the scaling in Fig. 7 are shown as function of the waiting time t_w . It can be seen that even if they could be fitted with power laws (with an exponent $\alpha \sim 0.38 \pm 0.1$ different from the exponent found for the Lennard-Jones case), the collapse of the different t_w curves is not good.

It is worth making a comparison of our numerical results with recent data measured by Pham *et al.*,²⁷ for a system of colloids with depletion interaction. In their experiment, the authors measure the density–density correlation function in the aging regime for two system at different polymer concentration, corresponding, respectively, to conditions where

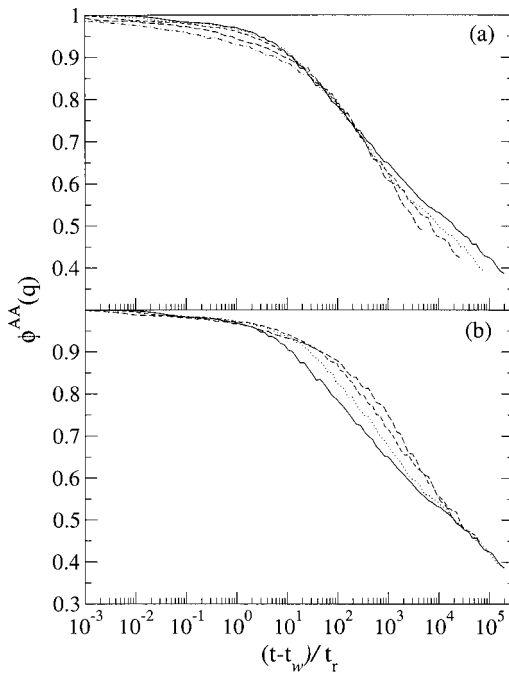


FIG. 7. Scaling of the density–density correlation functions for $T_f=0.3$. The waiting times are $t_w=10^1$ (continuous line), 10^2 (dotted line), 10^3 (short-dashed line), 10^4 (long-dashed line), 10^5 (dot-dashed line). (a) Best scaling for the region where $0.7 < \phi_q < 0.9$. (b) Best scaling for the region where $0.35 < \phi_q < 0.5$.

the repulsive and the attractive glass are expected. To better compare with Pham *et al.* data, we calculated the density dynamical structure factor (irrespective of the particle type) for the same q -vector of the cited experiment. Results are shown in Figs. 9 and 10 where the $T_f=1.2$ and $T_f=0.3$ quenches are, respectively, compared with the experimental results from Ref. 27 (lower panel). We present our results in seconds, after converting the numerical units $[\sigma \cdot (m/k_b T)^{1/2}]$ to physical units, as explained in the caption of Fig. 9. The difference in the time scale can be ascribed to the different microscopic dynamics implemented in the MD (Newtonian) as compared to the experimental one (Brownian). Slight differences in the plateau values can be ascribed to differences in the actual composition of the simulated (binary mixture) and experimental (slightly polydisperse system). The agreement between the numerical and the experimental data is impressive.

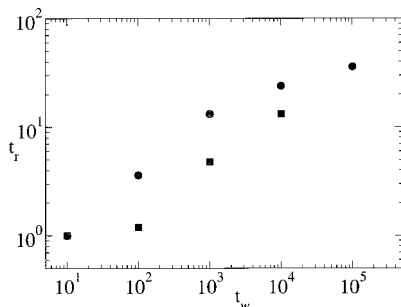


FIG. 8. Scaling coefficient used to obtain the scaling in Figs. 7(a) and 7(b). The circle are the scaling coefficient for the case in Fig. 7(a), the square for Fig. 7(b).

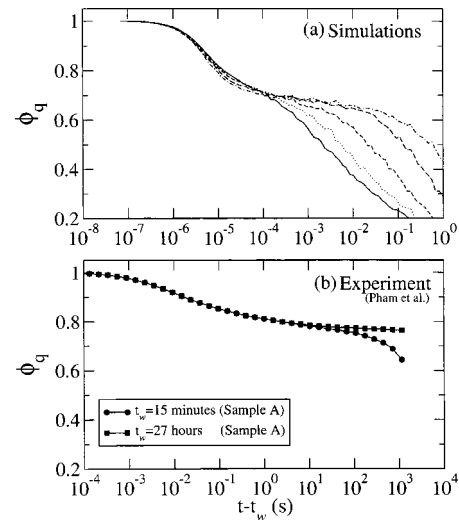


FIG. 9. Upper panel: total density–density correlation functions for $q\sigma_B = 2.93$ at different waiting times for $T_f=1.2$. From right to left, longer and longer relaxation time, $t_w=3.67 \times 10^{-4}$, 3.67×10^{-3} , 3.67×10^{-2} , 3.67×10^{-1} , 3.67×10^0 seconds. The unit of time $\sigma \cdot (m/u_0)^{1/2}$ used in the simulations has been converted to seconds using $m=4.1086 \times 10^{-17}$ Kg, $\sigma_A = 2.02 \times 10^{-7}$ m, and $u_0/k_b T = 1/1.2$ with T evaluated at ambient temperature, consistent with the experimental conditions. With this choice $\sigma \cdot (m/u_0)^{1/2} = 3.67 \times 10^{-5}$ seconds. Lower panel: experimental data reproduced from Ref. 27.

Another important two-time observable is the mean-squared displacement (MSD). In aging, it is defined as $\langle |\mathbf{r}(t-t_w) - \mathbf{r}(t_w)|^2 \rangle$, where $\mathbf{r}(t)$ is the position of the particle at time t and the average $\langle \cdot \rangle$ is performed over all the particles and the independent configurations. Here we focus on the total MSD, i.e., evaluated with no distinction between particles of the two species.

Figure 11(a) shows the MSD for $T_f=1.2$. In analogy with the case of the density correlators, at short times there is no significant t_w -dependence. At larger times the diffusive process is visible. When the waiting time becomes large, a plateau starts to emerge at intermediate times, between the

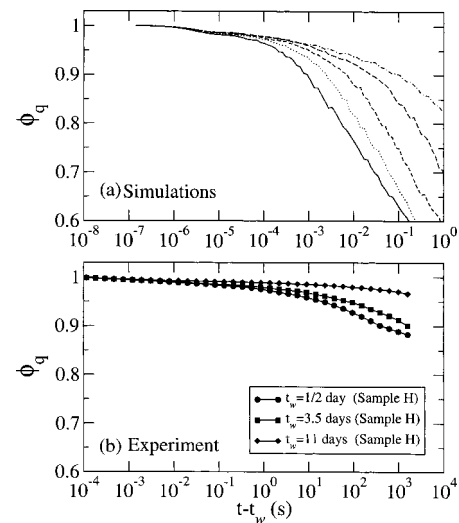


FIG. 10. Upper panel: same as in Fig. 9 for $T_f=0.3$. At this temperature $\sigma \cdot (m/u_0)^{1/2} = 7.34 \times 10^{-5}$. Lower panel: again experimental data are taken from Ref. 27.

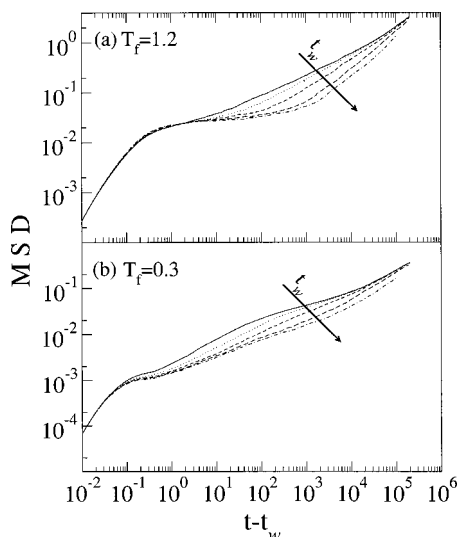


FIG. 11. (a) Mean-square displacement (MSD) for the quench at $T_f=1.2$ for increasing waiting times $t_w=10^1$ (continuous line), 10^2 (dotted line), 10^3 (short-dashed line), 10^4 (long-dashed line), 10^5 (dot-dashed line). (b) As in (a) for $T_f=0.3$.

ballistic (short time) and the diffusive (long time) regime. The duration of the plateau grows as t_w increases. As above, this behavior is similar to the one observed in previous simulations of a binary mixture of Lennard-Jones particles.²⁵

This three time-region behavior (ballistic, plateau, diffusive) is generally explained in term of the so called cage effect. When repulsive interactions start to be dominant the system slows down since each particle starts to get trapped in a shell of first neighbor particles. The length of the plateau indicates the typical time that a particle needs to escape this cage. The value of the plateau stands at the typical size of a cage, i.e., around 10% of the diameter in agreement with Lindemann's melting criterion.³⁸ For $T_f=0.3$, the MSD shows a completely different behavior [Fig. 11(b)]. Its evolution can again be divided in three time-regions, but now the short time (ballistic) and the long time (diffusive) regions bracket a long intermediate region where the MSD appears to grow as a power-law in time, with an effective exponent which decreases with t_w . Differently from the previous case, no evident sign of a plateau is present, except for a hint of a plateau at $\text{MSD}=0.001$ which starts to develop for large waiting times for $t-t_w \approx 0.5$. This value is consistent with a displacement of the order of the width of the potential well, and can be interpreted as a result of particles bonding in the attractive well, i.e., as some sort of attractive cages. However, activated bond-breaking processes appear to destroy such a confinement on time scales longer than $t-t_w \approx 1$.

IV. CONCLUSIONS

In systems with short-ranged attractive potentials, an efficient competition between attraction and excluded volume generates a highly nontrivial equilibrium dynamics and two kinetically distinct glasses. In the attractive glass, the particle localization is controlled by the bonding distance, while in the repulsive glass localization is controlled by the neighbor location. This offers the unique possibility of studying two

different aging dynamics within the same model. In this article, we have realized this numerically for a model system which shows both types of disordered arrested structures, the square well potential. We have found that the aging dynamics is clearly different for the two glasses, both in the waiting time evolution of the one-time quantities, and in the time evolution of the two-times quantities.

The results reported in this article refer to a simple model system which capture the essence of the physics introduced by the short-range attraction. The square well potential is indeed a satisfactory representation of the coarse-grained particle-particle potential in colloidal system, for example, in the presence of depletion interactions. Of course, dynamical features of the solvent constituents and of the solvent-particle interactions may significantly affect the particle dynamics. In this respect, the experimental validation of the equilibrium results is very valuable.

In particular, we have shown that the partial static structure factor evolves with t_w , showing opposite trends in the two cases, i.e., the first peak grows with t_w for the repulsive glass while decreases for the attractive one. We have also shown that the decay of correlation functions becomes slower and slower on increasing t_w in both cases, but with noteworthy differences in the strength of the relaxation (much more intense for the attractive glass case) and in the shape of the relaxation itself. The analysis of the MSD brings clear evidence that, while in the repulsive case there is the emergence of a plateau, whose time duration increases significantly with t_w , in the attractive glass case this does not happen. Indeed, in short-ranged attractive colloids, activated processes can be associated with thermal fluctuations of order u_0 , which allow particles to escape from the bonds. These processes generate a finite bond lifetime and, at the same time, may destabilize the attractive glass. It is important to find out how the difference in the aging dynamics arising from the different localization mechanisms are affected by the presence of activated processes.

Finally, we have shown that a good agreement is found between experimental and numerical data, also in the aging dynamic.

ACKNOWLEDGMENTS

We acknowledge support from MIUR COFIN 2002 and FIRB and from INFM Iniziativa Calcolo Parallelo. We thank W. C. K. Poon and K. N. Pham for useful discussion and for bringing their results to our attention.

¹P. N. Pusey, in *Liquids, Freezing and Glass Transition*, edited by J. P. Hansen, D. Levesque, and J. Zinn-Justin (North Holland, Amsterdam, 1991), Vol. Session LI (1989) of Les Houches Summer Schools of Theoretical Physics, pp. 765–942.

²A. P. Gast, W. Russell, and C. Hall, *J. Colloid Interface Sci.* **96**, 1977 (1983).

³E. Meijer and D. Frenkel, *Phys. Rev. Lett.* **67**, 1110 (1991).

⁴V. Anderson and H. Lekkerkerker, *Nature (London)* **416**, 811 (2002).

⁵F. Sciortino, *Nature Materials* **1**, 145 (2002).

⁶In fact the repulsive glass should be named more correctly “hard-sphere” glass, since this is the real nature of the repulsion in the system we shall study.

⁷W. Götze, in *Liquids, Freezing and Glass Transition*, edited by J. P. Hansen, D. Levesque, and J. Zinn-Justin (North Holland, Amsterdam,

- 1991), Vol. Session LI (1989) of Les Houches Summer Schools of Theoretical Physics, pp. 287–503.
- ⁸L. Fabbian, W. Götze, F. Sciortino, P. Tartaglia, and F. Thiery, *Phys. Rev. E* **59**, R1347 (1999).
- ⁹J. Bergenholtz and M. Fuchs, *Phys. Rev. E* **59**, 5706 (1999).
- ¹⁰K. Dawson, G. Foffi, M. Fuchs, W. Götze, F. Sciortino, M. Sperl, P. Tartaglia, T. Voigtmann, and E. Zaccarelli, *Phys. Rev. E* **63**, 011401 (2001).
- ¹¹G. Foffi, G. D. McCullagh, A. Lawlor, E. Zaccarelli, K. A. Dawson, F. Sciortino, P. Tartaglia, D. Pini, and G. Stell, *Phys. Rev. E* **65**, 031407 (2002).
- ¹²W. Götze and M. Sperl, *J. Phys.: Condens. Matter* **15**, S869 (2003).
- ¹³A. M. Puertas, M. Fuchs, and M. E. Cates, *Phys. Rev. Lett.* **88**, 098301 (2002).
- ¹⁴G. Foffi, K. A. Dawson, S. V. Buldyrev, F. Sciortino, E. Zaccarelli, and P. Tartaglia, *Phys. Rev. E* **65**, 050802(R) (2002).
- ¹⁵E. Zaccarelli, G. Foffi, K. A. Dawson, S. V. Buldyrev, F. Sciortino, and P. Tartaglia, *Phys. Rev. E* **66**, 041402 (2002).
- ¹⁶A. M. Puertas, M. Fuchs, and M. E. Cates, *Phys. Rev. E* **67**, 031406 (2003).
- ¹⁷F. Mallamace, P. Gambadauro, N. Micali, P. Tartaglia, C. Liao, and S.-H. Chen, *Phys. Rev. Lett.* **84**, 5431 (2000).
- ¹⁸K. N. Pham, A. M. Puertas, J. Bergenholtz, S. U. Egelhaaf, A. Moussaïd, P. N. Pusey, A. B. Schofield, M. E. Cates, M. Fuchs, and W. C. K. Poon, *Science* **296**, 104 (2002).
- ¹⁹T. Eckert and E. Bartsch, *Phys. Rev. Lett.* **89**, 125701 (2002).
- ²⁰S.-H. Chen, W.-R. Chen, and F. Mallamace, *Science* **300**, 619 (2003).
- ²¹W.-R. Chen, F. Mallamace, C. J. Glinka, E. Fratini, and S.-H. Chen, *Phys. Rev. E* **68**, 041402 (2003).
- ²²T. Eckert and E. Bartsch, *Faraday Discuss.* **123**, 51 (2003).
- ²³F. Sciortino, P. Tartaglia, and E. Zaccarelli, *Phys. Rev. Lett.* **91**, 268301 (2003).
- ²⁴E. Zaccarelli, G. Foffi, F. Sciortino, and P. Tartaglia, *Phys. Rev. Lett.* **91**, 108301 (2003).
- ²⁵W. Kob and J.-L. Barrat, *Phys. Rev. Lett.* **78**, 4581 (1997).
- ²⁶F. Sciortino and P. Tartaglia, *J. Phys.: Condens. Matter* **13**, 9127 (2001), and references therein.
- ²⁷K. N. Pham, S. U. Egelhaaf, P. N. Pusey, and W. C. K. Poon, *Phys. Rev. E* **69**, 011503 (2004).
- ²⁸D. C. Rapaport, *The art of computer simulations*, 2nd ed. (Cambridge University Press, London, 1997).
- ²⁹L. F. Cugliandolo and J. Kurchan, *Phys. Rev. Lett.* **71**, 173 (1993).
- ³⁰G. Parisi, *J. Phys. A* **30**, 8523 (1997).
- ³¹A. Latz, *J. Phys.: Condens. Matter* **12**, 6353 (2000).
- ³²F. Sciortino and P. Tartaglia, *Phys. Rev. Lett.* **86**, 107 (2001).
- ³³P. De Gregorio, F. Sciortino, P. Tartaglia, E. Zaccarelli, and K. Dawson, *Physica A* **307**, 15 (2002).
- ³⁴E. Zaccarelli, G. Foffi, K. A. Dawson, S. V. Buldyrev, F. Sciortino, and P. Tartaglia, *J. Phys.: Condens. Matter* **16**, S367 (2003).
- ³⁵G. Foffi, W. Götze, F. Sciortino, P. Tartaglia, and T. Voigtmann, *Phys. Rev. E* **69**, 011505 (2004).
- ³⁶L. F. Cugliandolo, lecture notes, Les Houches, July 2002, cond-mat/0210312.
- ³⁷T. S. Grigera, V. Martin-Mayor, G. Parisi, and P. Verrocchio, cond-mat/0307643.
- ³⁸N. W. Ashcroft and N. D. Mermin, *Solid state physics* (International Thomson, Washington, DC, 1976).
- ³⁹E. Zaccarelli, G. Foffi, P. D. Gregorio, F. Sciortino, P. Tartaglia, and K. A. Dawson, *J. Phys.: Condens. Matter* **14**, 2413 (2002).